

## Mts1 Regulates the Assembly of Nonmuscle Myosin-IIA<sup>†</sup>

Zhong-Hua Li, Anna Spektor, Olga Varlamova, and Anne R. Bresnick\*

*Department of Biochemistry, Albert Einstein College of Medicine, 1300 Morris Park Avenue, Bronx, New York 10461*

*Received August 12, 2003; Revised Manuscript Received October 2, 2003*

**ABSTRACT:** The formation of myosin-II filaments is fundamental to contractile and motile processes in nonmuscle cells, and elucidating the mechanisms controlling filament assembly is essential for understanding how myosin-II rapidly responds to changing conditions within the cell. Several proteins including KRP and a novel 38 kDa protein (*I*, 2) have been shown to modulate filament assembly through the stabilization of myosin-II assemblies. In contrast, we demonstrate that mts1, a member of the Ca<sup>2+</sup>-regulated S100 family of proteins, may regulate the monomeric, unassembled state in an isoform-specific manner. Biochemical analyses demonstrate that mts1 has a 9-fold higher affinity for myosin-IIA filaments than for myosin-IIB filaments. At stoichiometric levels, mts1 inhibits the assembly of myosin-IIA monomers into filaments and promotes the disassembly of myosin-IIA filaments into monomers; however, mts1 has little effect on the assembly properties of myosin-IIB. Using a solution based-assay, we have demonstrated that mts1 binds to residues 1909–1924 of the myosin-IIA heavy chain, which is near the C-terminal tip of the  $\alpha$ -helical coiled-coil. The observation that mts1 binds a linear sequence of ~16 amino acids is consistent with other S100 family members, which bind linear sequences of 13–22 residues in their protein targets. In addition, mts1 increases the critical monomer concentration for myosin-IIA filament assembly by approximately 11-fold. Kinetic assembly assays indicate that the elongation rate and the extent of polymerization depend on the initial myosin-IIA concentration; however, mts1 had only a small effect on the half-time for assembly and predominately affected the extent of myosin IIA polymerization. Altogether, these observations are consistent with mts1 regulating myosin IIA assembly by monomer sequestration and suggest that mts1 regulates cell shape and motility through the modulation of myosin-IIA function.

Mts1, which is also known as S100A4, FSP1, CAPL, calvasculin, metastasin, p9Ka, 18A2, and pEL98, is a member of the S100 family of Ca<sup>2+</sup>-binding proteins. At present, there are 21 known S100 family members, which generally form homodimers with total molecular masses ranging from 20 to 24 kDa. The S100 proteins have been implicated in the calcium-dependent regulation of a broad range of intracellular activities including substrate phosphorylation, the assembly/disassembly of cytoskeletal proteins, the modulation of enzyme activity, the regulation of cell cycle events, and calcium homeostasis (3). Importantly, most S100 family members display a high degree of target specificity, suggesting that individual S100 proteins regulate specific cellular processes.

While mts1 expression has been observed in normal tissues such as spleen and thymus, mts1 is expressed at elevated levels in motile cells such as macrophages, lymphocytes, and neutrophils (4). In addition, high mts1 expression has been observed in a number of metastatic cells. For example, metastatic rat and mouse mammary tumor cells express increased levels of mts1 as compared to nonmetastatic tumor cells (5). Similarly, mts1 expression is higher in malignant human breast tumors than in benign tumors (6) and correlates

strongly with poor patient survival (7, 8). Overexpression of mts1 in nonmetastatic rat and mouse mammary tumor cells confers a metastatic phenotype (9, 10), whereas in metastatic cells, a reduction in mts1 expression suppresses metastatic potential (11, 12). Transgenic mice that overexpress mts1 in the mammary epithelium are phenotypically indistinguishable from wild-type mice (13), demonstrating that mts1 itself is not tumorigenic; however, transgenic mouse models of breast cancer have shown that mts1 expression correlates with metastasis (13, 14). These findings suggest a significant role for mts1 in promoting the metastatic phenotype.

The first evidence indicating a functional role for mts1 in the metastatic phenotype came from immunoprecipitation studies demonstrating that mts1 immunoprecipitates from [<sup>35</sup>S]-radiolabeled metastatic mammary cells contain myosin-II (15). More recent studies have shown that mts1 directly binds nonmuscle myosin-II in a Ca<sup>2+</sup>-dependent manner (16, 17) and that binding inhibits the actin-activated ATPase activity of myosin-II (16). In addition, mts1 has been shown to bind actin (18) and tropomyosin (19) in a Ca<sup>2+</sup>-dependent manner in vitro. These binding interactions are consistent with the observation that mts1 expression levels correlate strongly with the motility of tumors cells (20) and suggest a direct link between the actomyosin cytoskeleton and the regulation of cellular motility by mts1.

To further characterize the regulation of nonmuscle myosin-II by mts1, we examined the isoform specificity of

<sup>†</sup> This work was supported by the Department of Defense Breast Cancer Research Program (DAMD17-01-1-0122).

\* To whom correspondence should be addressed. Telephone: (718) 430-2741. Fax: (718) 430-8565. E-mail: bresnick@aecom.yu.edu.

the mts1–myosin-II interaction and the modulation of myosin-II assembly by mts1. Our findings support a model in which mts1 regulates cell shape and motility by controlling the assembly state of myosin-II filaments.

## EXPERIMENTAL PROCEDURES

**Protein Purification.** Rabbit skeletal muscle actin was purified from acetone powder by the method of Spudich and Watt (21). Recombinant human mts1 was purified as described previously (22).

**Bacterial Expression and Purification of Myosin-IIA and Myosin-IIB Rods.** The human myosin-IIA and myosin-IIB rods were subcloned into the Nde I/Bam HI sites of the expression vector pET28a (Novagen). The N-terminus of each construct contains MGSSHHHHHSSGLVPRGSHM followed by residues 1339–1961 of the human myosin-IIA heavy chain (23, 24) or residues 1346–1976 of the human myosin-IIB heavy chain (25). The final constructs were verified by DNA sequencing. BL21(DE3) cells transformed with either hMIIA-pet28a or hMIIB-pet28a were grown overnight at 37 °C. The cells were harvested at 15 000g for 10 min, and the cell pellet was resuspended in 7.5 mL of lysis buffer/gram of cell pellet (lysis buffer: 50 mM Tris, 5 mM EDTA, 5% sucrose, 1 M NaCl, 1 mM DTT, 0.02% NaN<sub>3</sub>, 0.3 mM PMSF, and 5 µg/mL each of chymostatin, leupeptin, and pepstatin). The cell lysate was sonicated for 8 × 10 s on ice, boiled for 25 min, and cooled on ice for 20 min. Following centrifugation of the boiled lysate at 27 000g for 15 min, ammonium sulfate was added to the supernatant to 65% saturation, and the sample was centrifuged at 17 000g for 20 min. The pellet was resuspended in buffer E (buffer E: 20 mM Tris pH 7.5, 2 mM EDTA, 6 M urea, 0.5 mM DTT, 0.02% NaN<sub>3</sub>) and applied to a High Q Sepharose column equilibrated in buffer E. The column was washed with 2 column volumes of buffer E, and the myosin rods eluted in the flow through. The myosin rods were assembled by dialysis against 5 mM PIPES pH 6.5, 20 mM NaCl, 10 mM MgCl<sub>2</sub>, 1 mM DTT, 0.02% NaN<sub>3</sub>, collected by centrifugation at 15 000g for 20 min and disassembled by dialysis against Tris pH 7.5, 0.6 M NaCl, 1 mM DTT, 0.02% NaN<sub>3</sub>. Typical protein yields were 50 mg of myosin rods per liter of cells.

**Purification of GST-Myosin-IIA Peptide Fusions.** The cDNAs corresponding to residues 1900–1961, 1909–1940, 1909–1924, 1917–1932, and 1925–1940 of the human myosin-IIA heavy chain were subcloned into the Bam HI/Eco RI sites of pGEX-6P-1 (Pharmacia). All the constructs contain GST<sup>1</sup> followed by LEVLFQGPLGS and the appropriate myosin-IIA heavy chain sequence, which were verified by DNA sequencing. A control GST was prepared by introducing a stop codon immediately after the Bam HI site in pGEX-6P-1. The resulting control GST contained the PreScission protease recognition sequence and the linker sequence present in the GST-myosin-IIA peptide fusions. BL21(DE3) cells transformed with the GST-myosin-IIA peptides or the control GST were induced with 1 mM IPTG and grown at 37 °C for 6 h. The cells were harvested at 15 000g for 10 min, and the cell pellet was resuspended in

7 mL of lysis buffer/gram of cell pellet (lysis buffer: 50 mM Tris pH 8.0, 20% sucrose, 200 mM NaCl, 1 mM EDTA, 2 mM DTT, 1 mM PMSF, and 5 µg/mL each of chymostatin, leupeptin, and pepstatin). The cell lysate was frozen at –70 °C, thawed on ice, and sonicated for 6 × 15 s on ice. Following centrifugation at 31 000g for 20 min, the supernatant was applied to a glutathione-Sepharose column equilibrated in cleavage buffer (50 mM Tris pH 7.5, 150 mM NaCl, 1 mM DTT, 1 mM EDTA, 0.02% NaN<sub>3</sub>), and the column washed with 25 column volumes of cleavage buffer. The GST fusions were eluted with 50 mM Tris pH 8.0, 1 mM DTT, and 10 mM reduced glutathione and loaded onto a Mono Q column equilibrated in buffer Q (20 mM Tris pH 7.5, 20 mM NaCl, 0.5 mM DTT, 0.02% NaN<sub>3</sub>). The column was washed with 2 column volumes of buffer Q and developed with a 10 column volume linear gradient of 0.02–1.0 M NaCl in buffer Q. Typical yields were 3–15 mg of GST-myosin-IIA peptide per liter of cells, depending on the particular construct. The molecular weights of the GST-myosin-IIA peptides were confirmed by mass spectrometry.

**Cosedimentation Assays.** For the myosin rod binding assays, myosin-IIA or myosin-IIB rods (final concentration of 6 µM) were added to a reaction mix containing 1–200 µM mts1 dimer in 20 mM Tris pH 7.5, 20 mM NaCl, 2 mM MgCl<sub>2</sub>, 0.3 mM CaCl<sub>2</sub>, 1 mM DTT, 0.02% NaN<sub>3</sub> for 30 min at room temperature in the presence or absence of 2 mM EGTA. Samples were centrifuged at room temperature for 20 min at 100 000g (20 psi) in a Beckman airfuge (Beckman). Samples of the supernatants and pellets were separated on a 12% Tricine SDS–polyacrylamide gel. Gels were scanned on a model GS-700 BioRad Imaging densitometer and quantified using the program ImageQuant version 5.0. F-actin binding assays were performed as described for myosin rod binding assays using a final concentration of 10 µM actin. The binding constants and stoichiometry of binding were calculated by fitting the data to the equation  $b = \frac{B_{\max}[S]}{K_d + [S]}$ .

**Inhibition of Filament Assembly by Mts1.** Monomeric myosin rods (3 µM) were added to a reaction mix containing 0–36 µM mts1 dimer in 20 mM Tris pH 7.5, 300 mM NaCl, 1 mM DTT, 2 mM MgCl<sub>2</sub>, 0.3 mM CaCl<sub>2</sub>, 0.02% NaN<sub>3</sub> for 15 min at room temperature. A sample of the mix was removed for SDS–PAGE analysis, and the final reaction mixture was diluted with an equal volume of 20 mM Tris pH 7.5, 1 mM DTT, 2 mM MgCl<sub>2</sub>, 0.3 mM CaCl<sub>2</sub>, 0.02% NaN<sub>3</sub>, yielding a final concentration of 150 mM NaCl, 1.5 µM myosin rods, and 0–18 µM mts1 dimer. The mixtures were incubated for 1 h at room temperature and centrifuged at 80 000 rpm (175 000g) for 10 min at 25 °C in a TL-100 ultracentrifuge (Beckman). Mixes and supernatants were separated on a 12% Tricine SDS–polyacrylamide gel, scanned as described previously, and quantified using the program ImageQuant version 5.0.

**Promotion of Filament Disassembly by Mts1.** Filamentous myosin rods (3 µM) were added to a reaction mix containing 0–36 µM mts1 dimer in 20 mM Tris pH 7.5, 150 mM NaCl, 1 mM DTT, 2 mM MgCl<sub>2</sub>, 0.3 mM CaCl<sub>2</sub>, 0.02% NaN<sub>3</sub> for 15 min at room temperature. A sample of the mix was removed for SDS–PAGE analysis, and the final reaction mixture was incubated at room temperature for an additional 45 min. The mixtures were centrifuged at 80 000 rpm

<sup>1</sup> Abbreviations: GST, glutathione S-transferase; MIIA, myosin-IIA; ACD, assembly competence domain; RLC, regulatory light chain; PKC, protein kinase C.

(175 000g) for 10 min at 25 °C in a TL-100 ultracentrifuge (Beckman). Mixes and supernatants were analyzed as described previously for assays examining the inhibition of assembly.

**Glutathione Bead Copelleting Assay.** The 10  $\mu$ M mts1 dimer was mixed with 10  $\mu$ M GST-MIIA peptides or the control GST bound to glutathione-Sepharose in 20 mM Tris pH 7.5, 50 mM NaCl, 0.5 mM DTT, 0.3 mM CaCl<sub>2</sub>, 0.02% NaN<sub>3</sub>, and 0.5 mg/mL BSA in the presence or absence of 2 mM EGTA for 1 h at room temperature. The mixtures were centrifuged at 5000g for 2 min, and the supernatants were removed. The pellets were washed three to four times in binding buffer and resuspended in Laemmli sample buffer for analysis on a 12% Tricine SDS–polyacrylamide gel. To determine equilibrium dissociation constants, 0–40  $\mu$ M mts1 dimer was mixed with 10  $\mu$ M GST-myosin-IIA peptides or the control GST bound to glutathione-Sepharose in 20 mM Tris pH 7.5, 50 mM NaCl, 0.5 mM DTT, 0.3 mM CaCl<sub>2</sub>, 0.02% NaN<sub>3</sub>, and 0.167 mg/mL BSA. Samples of the pellets were analyzed on a 12% Tricine SDS–polyacrylamide gel, and the staining intensity of the mts1 was compared with a standard curve of purified recombinant human mts1 run on the same gel. Wet gels were scanned, and the amount of bound mts1 was quantified using the program ImageQuant version 5.0. The binding constants and stoichiometry of binding were calculated by fitting the data to the equation  $b = B_{\max}[S]/(K_d + [S])$ .

**Competition Assays.** The 6  $\mu$ M myosin-IIA rods, 6  $\mu$ M mts1 dimer, and 0–150  $\mu$ M GST-myosin-IIA peptides (GST-MIIA<sub>1909–1940</sub>, GST-MIIA<sub>1925–1940</sub>, and GST-MIIA<sub>1909–1924</sub>) were mixed in a buffer containing 20 mM Tris pH 7.5, 20 mM NaCl, 2 mM MgCl<sub>2</sub>, 0.3 mM CaCl<sub>2</sub>, 1 mM DTT, 0.02% NaN<sub>3</sub>. After incubation at room temperature for 30 min, the mixture was centrifuged 80 000 rpm for 10 min at 25 °C in a TL-100 ultracentrifuge (Beckman). Samples of the pellets were analyzed on a 12% Tricine SDS–polyacrylamide gel, and the amount of bound mts1 was determined as described previously for the glutathione bead copelleting assay.

**Critical Concentration Measurements.** Myosin-IIA rods were adjusted to different starting concentrations (0–80  $\mu$ M) in storage buffer (20 mM Tris pH 7.5, 0.6 M NaCl, 1 mM DTT, 0.02% NaN<sub>3</sub>) and then quickly diluted 4-fold using a buffer containing 20 mM Tris pH 7.5, 1 mM DTT, 0.02% NaN<sub>3</sub>, 0.4 mM CaCl<sub>2</sub>, and 2.67 mM MgCl<sub>2</sub>. The final buffer contained 150 mM NaCl, 0.3 mM CaCl<sub>2</sub>, 2 mM MgCl<sub>2</sub>, and 0–20  $\mu$ M myosin-IIA rods. After incubation at room temperature for 30–60 min, the samples were centrifuged at 95 000 rpm for 15 min at 4 °C in a TL-100 ultracentrifuge (Beckman). Aliquots of the mix before centrifugation and the supernatant after centrifugation were removed for SDS–PAGE analysis. To determine the effect of mts1 on the critical concentration for myosin-IIA filament assembly, the myosin-IIA rods (0–80  $\mu$ M) were incubated with 8–40  $\mu$ M mts1 dimer for ~45 min in storage buffer containing 0.3 mM CaCl<sub>2</sub> before dilution with 20 mM Tris pH 7.5, 1 mM DTT, 0.02% NaN<sub>3</sub>, 0.3 mM CaCl<sub>2</sub>, and 2.67 mM MgCl<sub>2</sub>. Following dilution, the concentration of the myosin-IIA rods and mts1 was 0–20 and 0–10  $\mu$ M, respectively. Samples of the mixes and supernatants were analyzed on a 12% Tricine SDS–polyacrylamide gel, and the staining intensity of the myosin-IIA was compared with a standard curve of purified recombinant myosin-IIA rods run on the same gel.

The amount of monomeric myosin-IIA in each supernatant was plotted as a function of the total myosin-IIA. The data were fitted with the linear equation  $y = mx + b$  for the plateau values of  $x$  as described previously (26).

**Myosin Assembly Assays.** Turbidity, measured in a UV-2401 PC UV–vis spectrophotometer (Shimadzu Scientific Instruments, Inc.), was used to monitor the kinetics of myosin-IIA assembly. Previous studies with skeletal and *Dictyostelium* myosin-II have shown that turbidity is linearly proportional to the myosin-II concentration and that the apparent half-times obtained from turbidometric measurements accurately reflect the assembly of 50% of the myosin into thick filaments (27, 28). For all assays, turbidity was monitored at 320 nm with a slit width of 2 nm at room temperature (~25 °C). All buffers were filtered using a 0.22  $\mu$ m filter (Nanopure) and degassed. Polymerization was induced by a rapid 4-fold dilution of a 2–40  $\mu$ M solution of myosin-IIA rods in 20 mM Tris pH 7.5, 0.6 M NaCl, 1 mM DTT, 0.02% NaN<sub>3</sub> into a buffer containing 20 mM Tris pH 7.5, 2.67 mM MgCl<sub>2</sub>, 1 mM DTT, 0.02% NaN<sub>3</sub>, and 0.4 mM CaCl<sub>2</sub>, yielding a final concentration of 150 mM NaCl, 2 mM MgCl<sub>2</sub>, and 0.3 mM CaCl<sub>2</sub>. To examine the effect of mts1 on myosin-IIA assembly, 20  $\mu$ M myosin-IIA rods were incubated with 2–20  $\mu$ M mts1 dimer for 30 min in 20 mM Tris pH 7.5, 0.6 M NaCl, 1 mM DTT, 0.02% NaN<sub>3</sub>, 0.3 mM CaCl<sub>2</sub> and then diluted 4-fold to induce polymerization. The 200  $\mu$ L samples were prepared by manual dilution and read in a 50  $\mu$ L micro cell quartz cuvette for 30 min. The first reading was taken after the cuvette was returned to the chamber following dilution. Assembly half-times ( $t_{1/2}$ ) were determined from manual dilution experiments by fitting the data to a single-exponential  $y = y_0 + a(1 - e^{-bx})$ . Fits did not include data prior to 5 min since the interval between the manual dilution and the first reading ranged from 1 to 2 min. An overall apparent rate constant for assembly was derived from the half-time of assembly using the relationship  $t_{1/2} = (1/k_{\text{app}})(1/[M]_{t_{1/2}})$  for second-order reactions (29), where  $[M]_{t_{1/2}}$  is the concentration of unassembled myosin-II at  $t_{1/2}$ . For each myosin-IIA rod and mts1 concentration, three to five independent experiments were performed.

## RESULTS

**Binding of Mts1 to Cytoskeletal Elements.** Mts1 has been reported to bind both myosin-IIA and myosin-IIB (16) as well as actin (18). To assess the specificity of these interactions, we measured equilibrium dissociation constants ( $K_d$ ) for mts1 binding to these filamentous proteins. Myosin-II binding studies were performed at low ionic strength (i.e., 20 mM NaCl), as these conditions are known to enhance the stability of the myosin filaments. In contrast with the observations of Ford et al. (16), we did not detect any depolymerization of the myosin-II filaments under the ionic conditions used to assay mts1 binding (data not shown). Mts1 displayed a 9-fold higher affinity for myosin-IIA filaments than for myosin-IIB filaments and also showed a weak Ca<sup>2+</sup>-dependent interaction with actin (Table 1, Figure 1). Mts1 binding to myosin-II was not detected in the presence of EGTA, thus demonstrating that the interaction of mts1 with myosin-II has a strict requirement for Ca<sup>2+</sup>. The stoichiometry of binding to both myosin-II isoforms was 1 mol of mts1 dimer per three dimeric myosin-II rods (0.35 and 0.38 for myosin-IIA and myosin-IIB, respectively). These obser-



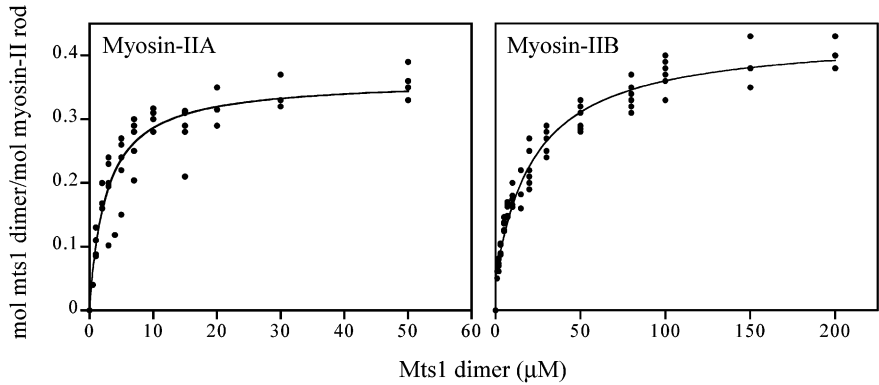


FIGURE 1: Binding of mts1 to myosin-II. Mts1 was cosedimented with either myosin-IIA or myosin-IIB rods at pH 7.5, 20 mM KCl, 2 mM MgCl<sub>2</sub>, and 0.3 mM CaCl<sub>2</sub>. The mol of mts1 dimer bound/mol of myosin rod was determined for each mts1 concentration.

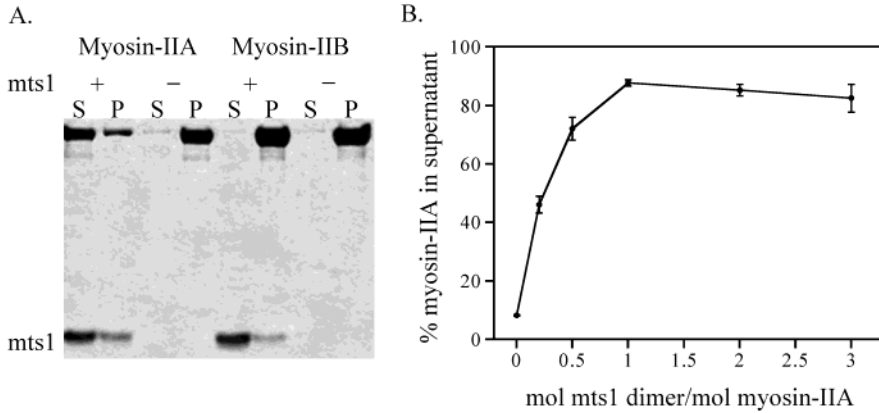


FIGURE 2: Mts1 promotes the disassembly of preformed myosin-IIA filaments in a Ca<sup>2+</sup>-dependent manner. (A) SDS-PAGE of myosin-IIA disassembly monitored in a standard pelleting assay. At physiological ionic strengths, the myosin-IIA filaments (3 μM) are found predominantly in the pellet. In the presence of 9 μM mts1 dimer, the disassembled filaments are found in the supernatant. Mts1 had no effect on the stability of the myosin-IIB filaments. (B) Maximal promotion of disassembly was observed at 1 mol of mts1 dimer/mol of myosin-IIA rod. Assays were performed using a pH 7.5 buffer containing 150 mM KCl, 2 mM MgCl<sub>2</sub>, and 0.3 mM CaCl<sub>2</sub>. Values represent the mean and standard error of the mean for three independent experiments.

Table 1: Relative Affinity of Mts1 for Cytoskeletal Elements<sup>a</sup>

	K <sub>d</sub> (μM)	
	+Ca <sup>2+</sup>	-Ca <sup>2+</sup>
myosin-IIA	2.7 ± 0.6	not detected
myosin-IIB	23.1 ± 2.7	not detected
F-actin	34.0 ± 6.2	543 ± 274

<sup>a</sup> Values represent the mean and standard deviation of the mean for three to five independent experiments.

vations suggest that close packing of the myosin-II rods in the filamentous state prevents a 1:1 binding stoichiometry.

**Regulation of the Myosin-II Monomer-Polymer Equilibrium by Mts1.** Under the conditions of our equilibrium binding studies, we did not detect any destabilization of the myosin-II filaments (i.e., the appearance of myosin in the supernatant with increasing mts1 concentrations). Since previous studies have suggested that mts1 destabilizes myosin filaments at moderate ionic strength (50 mM NaCl) (16), we assessed the ability of Ca<sup>2+</sup>-bound mts1 to promote filament disassembly at physiological ionic strengths (i.e., 150 mM NaCl). At a molar ratio of one mts1 dimer per myosin-IIA rod, we observed maximal disassembly with ~85% of the myosin-IIA in the supernatant (Figure 2). Over the range of mts1 concentrations that were used in this assay, we did not observe any effect on myosin-IIB filaments (Figure 2A). Since mts1 promoted the disassembly of

preformed myosin-IIA filaments, we next assessed whether mts1 binding had any effect on the assembly of myosin-II monomers into filaments. At a molar ratio of one mts1 dimer per myosin-IIA rod, we observed maximal inhibition of assembly with ~77% of the myosin-IIA remaining in the supernatant (Figure 3). In contrast, mts1 had only a minor effect on the assembly of myosin-IIB filaments (Figure 3A). These biochemical studies demonstrate that mts1 shifts the monomer-polymer equilibrium of myosin-II toward the monomeric, unassembled state and also suggest that mts1 may preferentially regulate myosin-IIA activity in vivo.

**Mapping the Mts1 Binding Site on the Myosin-IIA Rod.** Blot overlay analysis initially implicated the light mero-myosin region of the myosin rod as containing the mts1 binding site (16), and additional blot overlays demonstrated a loss of mts1 binding upon internal deletion of residues 1909–1937 of the myosin-IIA heavy chain (30). To confirm and extend these studies, we established a quantitative glutathione-Sepharose pull-down assay to map the mts1 binding site on the myosin-IIA heavy chain (Figure 4). Mts1 displayed Ca<sup>2+</sup>-dependent binding to GST-myosin-IIA peptides containing residues 1900–1961, 1909–1940, and 1909–1924 with equilibrium dissociation constants that were comparable to that observed for binding to the myosin-IIA rod (Tables 1 and 2) and binding stoichiometries of 0.83, 0.89, and 0.98 mol of mts1 dimer/mol of myosin-IIA peptide,

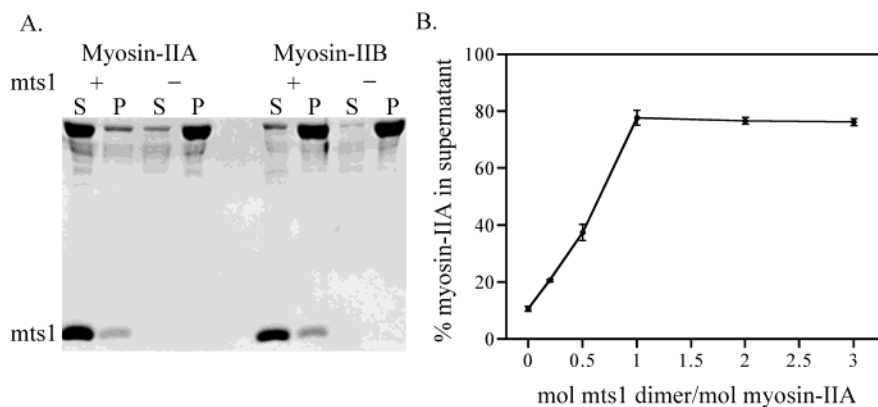


FIGURE 3: Mts1 selectively inhibits the assembly of myosin-IIA monomers in a  $\text{Ca}^{2+}$ -dependent manner. (A) SDS-PAGE of myosin-II assembly monitored in a standard pelleting assay. (A) At physiological ionic strengths, the assembled myosin-IIA filaments ( $3 \mu\text{M}$ ) are found predominantly in the pellet. In the presence of  $9 \mu\text{M}$  mts1 dimer, myosin-IIA oligomerization is inhibited, and the monomers remain in the supernatant. Mts1 had only a modest effect on the assembly of myosin-IIB filaments. (B) Maximal inhibition of assembly was observed at 1 mol of mts1 dimer/mol of myosin-IIA rod. Assays were performed using a pH 7.5 buffer containing 150 mM KCl, 2 mM  $\text{MgCl}_2$ , and 0.3 mM  $\text{CaCl}_2$ . Values represent the mean and standard error of the mean for three to six independent experiments.

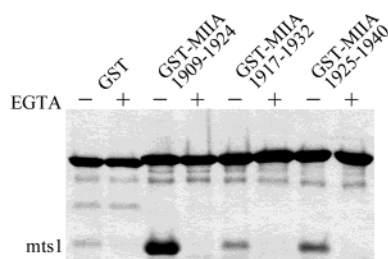


FIGURE 4: Mts1 binds residues 1909–1924 of the myosin-IIA heavy chain. A Coomassie-stained SDS-polyacrylamide gel showing samples of the GST fusion proteins immobilized on glutathione-Sepharose and bound mts1. Assays were performed using a pH 7.5 buffer containing 50 mM NaCl and 0.3 mM  $\text{CaCl}_2$ . Mts1 displays  $\text{Ca}^{2+}$ -dependent binding to a GST fusion containing residues 1909–1924 of the myosin-IIA heavy chain. Mts1 showed weak  $\text{Ca}^{2+}$ -dependent binding to residues 1917–1932 and residues 1925–1940 of the myosin-IIA heavy chain.

Table 2: Mts1 Binding Site on the Myosin-IIA Rod<sup>a</sup>

GST-MIIA peptide	$K_d$ ( $\mu\text{M}$ )
1900–1961	$3.59 \pm 0.53$
1909–1940	$3.11 \pm 0.58$
1909–1924	$6.57 \pm 0.84$
1917–1932	$240 \pm 23.0$
1925–1940	$95.3 \pm 7.5$
GST alone	$2961 \pm 493$

<sup>a</sup> Values represent the mean and standard deviation of the mean for three independent experiments.

respectively. Mts1 did not bind to GST alone in either the presence of  $\text{Ca}^{2+}$  or the presence of EGTA (Figure 4 and Table 2).

To confirm that residues 1909–1924 comprise the mts1 binding site on the myosin-IIA heavy chain, we performed a competition assay to determine if GST-myosin-IIA peptides containing this sequence inhibit the binding of mts1 to the myosin-IIA rods. The GST-myosin-IIA peptide containing residues 1925–1940 had no effect on the binding of mts1 to the myosin-IIA rods; however, for GST fusions containing peptides 1909–1940 and 1909–1924, half-maximal inhibition occurred at approximately  $36 \mu\text{M}$  peptide (Figure 5). These observations indicate that residues 1909–1924 of the myosin-IIA heavy chain are sufficient to bind mts1.

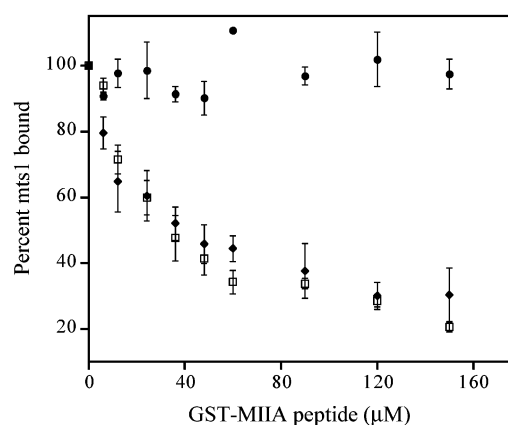


FIGURE 5: GST-myosin-IIA peptides containing residues 1909–1924 of the myosin-IIA heavy chain inhibit the binding of mts1 to myosin-IIA rods. Competition assays were performed at pH 7.5 in a buffer containing 20 mM NaCl, 2 mM  $\text{MgCl}_2$ , and 0.3 mM  $\text{CaCl}_2$ ; (●) GST-myosin-IIA peptide<sub>1925-1940</sub>, (□) GST-myosin-IIA peptide<sub>1909-1940</sub>, and (◆) GST-myosin-IIA peptide<sub>1909-1924</sub>. Values represent the mean and standard error of the mean for three independent experiments.

**Effect of Mts1 on Steady-State Myosin-IIA Polymerization.** To determine if mts1 affects the critical monomer concentration for myosin-IIA assembly, we measured the amount of rod monomer in equilibrium with rod polymer in the absence and presence of mts1. At pH 7.5 and 150 mM KCl and 2 mM  $\text{MgCl}_2$ , the amount of soluble myosin-IIA rods plateaued at  $0.20 \mu\text{M}$  ( $\sim 30 \mu\text{g/mL}$ ) monomer, indicating that this was the critical monomer concentration for filament assembly (Figure 6 and Table 3). This value is consistent with the critical concentrations observed for the full-length chicken myosin-IIA (31) and for rod fragments of the chicken smooth muscle SM-1 isoform (26), which has a nonhelical tailpiece similar to that found in myosin-IIA (32). In the absence of mts1, the slope of the plot of the sedimented myosin ( $C_p$ ) versus the total myosin ( $C_t$ ) was  $\sim 1$  (Table 3), indicating that above the critical concentration, the same concentration of myosin monomer is in equilibrium with polymer. At all mts1 concentrations examined, myosin-IIA polymerization was inhibited due to a  $\sim 11$ -fold increase in the critical monomer concentration (Figure 6 and Table 3). In addition, mts1 had a large effect on the amount of myosin-IIA that

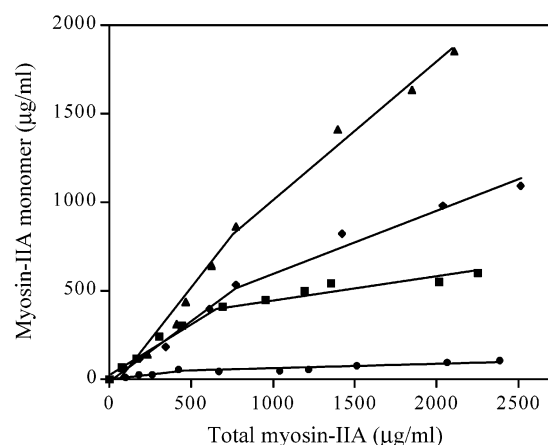


FIGURE 6: Mts1 regulates the critical monomer concentration for myosin-IIA assembly. The critical concentration for the myosin-IIA rods was assayed at pH 7.5 in 150 mM KCl, 2 mM MgCl<sub>2</sub>, and 0.3 mM CaCl<sub>2</sub> in the absence or presence of mts1. (●) No added mts1, (■) 2  $\mu$ M mts1, (◆) 5  $\mu$ M mts1, and (▲) 10  $\mu$ M mts1. Values represent the mean for two to four independent experiments.

Table 3: Effect of Mts1 on the Critical Concentration for Myosin-IIA Polymerization<sup>a</sup>

Mts1 ( $\mu$ M)	observed critical concentration ( $\mu$ M)	slope $C_p$ vs $C_t$
0	0.20	0.96
2	2.41	0.89
5	2.18	0.64
10	2.27	0.10

<sup>a</sup> Values represent the mean for two to four independent experiments.

polymerized above this higher critical concentration as plots of the polymer concentration ( $C_p$ ) versus the total myosin concentration ( $C_t$ ) yielded slopes  $<1$ . The slopes of the  $C_p$  versus  $C_t$  plots were inversely proportional to the mts1 concentration (Table 3), demonstrating the inhibitory effect of mts1 on myosin-IIA polymerization.

**Effect of Mts1 on the Kinetics Myosin-IIA Assembly.** We used continuous turbidity measurements to examine the kinetics of myosin-IIA assembly (Figure 7A). A plot of  $t_{1/2}$  versus  $1/[M_{t/2}]$ , where  $[M_{t/2}]$  is the concentration of un-assembled myosin-II at  $t_{1/2}$ , produced a linear fit to the second-order rate equation  $t_{1/2} = (1/k_{app})(1/[M_{t/2}])$ , which allowed an overall rate constant ( $k_{obs}$ ) of  $1.37 \times 10^4 \text{ M}^{-1} \text{ s}^{-1}$  to be calculated for the assembly of the myosin-IIA rods. This value is considerably slower than the rate constants obtained for the assembly of full-length skeletal myosin-II ( $k_{obs} = 3.3 \times 10^5 \text{ M}^{-1} \text{ s}^{-1}$ ) (33) and *Acanthamoeba* myosin-II ( $k_{obs} > 10^8 \text{ M}^{-1} \text{ s}^{-1}$ ) (34). The slow assembly of the recombinant myosin-IIA rods may be attributable to several causes. The myosin-IIA rods utilized in the present study comprise only the C-terminal half of the full-length myosin-IIA rod. Moreover, the rods contain a hexahistidine tag and a small linker at their N-termini, which may cause fraying at the N-terminal end of the coiled-coil and thus affect assembly. However, the assembly kinetics of our myosin-IIA rods are in fact comparable to the rate constant obtained for the assembly of full-length *Dictyostelium* myosin-II ( $k_{obs} = 2.5 \times 10^4 \text{ M}^{-1} \text{ s}^{-1}$ ) (28). Nevertheless, we were able to use this assay to examine how mts1 affects the overall rate constant for myosin-IIA assembly. For 5  $\mu$ M myosin-IIA

rods in the absence of mts1, we observed an assembly half-time ( $t_{1/2}$ ) of  $8.09 \pm 0.09 \text{ min}$ . The addition of mts1 at concentrations ranging from 0.5 to 1.5  $\mu$ M only increased the half-time for assembly by 12% ( $t_{1/2} = 9.06 \pm 0.15 \text{ min}$ ), suggesting that at low stoichiometries mts1 had little effect on the overall rate constant for myosin-IIA assembly. However, at these concentrations, mts1 decreased the amount of polymerized myosin-II by 17–55% (Figure 7B). Only at high molar ratios (i.e., 0.5 mts1 dimers per myosin-IIA rod) did we observe a significant effect on both the half-time for assembly ( $t_{1/2} = 13.29 \pm 0.39 \text{ min}$ ) and the final extent of polymerization (Figure 7B).

## DISCUSSION

Vertebrate nonmuscle cells express two myosin-II heavy chain isoforms (A and B) that are well-conserved except for their extreme C-termini or the so-called nonhelical tailpiece (23–25). Despite a high level of conservation, myosin-IIA and myosin-IIB display different enzymatic activities, show isoform-specific differences in the regulation of their assembly by heavy chain phosphorylation, and exhibit distinct patterns of localization (35–38), suggesting that the two isoforms may have unique functional roles in vivo.

For the first time, we have demonstrated quantitative differences in the interaction of mts1 with the nonmuscle myosin-II isoforms. In equilibrium binding studies, mts1 had 9-fold higher affinity for myosin-IIA filaments than for myosin-IIB filaments. We observed a  $K_d$  of 2.7  $\mu$ M for the binding of untagged mts1 to myosin-IIA rods, which is roughly comparable with the findings of Ford et al., who determined an approximate  $K_d$  of 12.6  $\mu$ M for the binding of a GST-mts1 fusion to the full-length myosin-IIA (16). Moreover, at low ionic strengths, our studies indicated an approximate stoichiometry of 1 mol of mts1 dimer per three dimeric myosin-II rods, which differs from the previously reported stoichiometry of 3 mol of mts1 monomer per dimeric myosin-II (16). This discrepancy may be a consequence of the GST-mts1 fusion used in earlier studies; since both mts1 and GST are dimers, the formation of higher order GST-mts1 aggregates may have complicated the stoichiometric determination.

In addition, our studies indicate that at physiological ionic strengths, mts1 preferentially regulates the monomer–polymer equilibrium of myosin-IIA. At stoichiometries of 1 mol of mts1 dimer per mol of myosin rod, mts1 binding caused maximal inhibition of both myosin-IIA assembly and disassembly of preformed myosin-IIA filaments. These findings contrast with those of Murakami et al., who reported that maximal inhibition of myosin-IIA assembly as well as the dissociation of myosin-IIA filaments occurred at stoichiometries greater than 2 mol of mts1 dimer per mol of myosin rod (39). The reduced activity of the mouse mts1 used in these earlier studies as compared to the human mts1 used in the present analysis may result from the presence of an N-terminal hexahistidine tag on the mouse mts1 and/or the pH 4.0 buffer used to elute protein off of the Ni-NTA resin.

The intracellular concentration of myosin-II in nonmuscle cells is  $\sim 1 \text{ mg/mL}$  or 2  $\mu$ M (40). Under approximately physiological conditions in vitro, we determined a critical monomer concentration of 0.20  $\mu$ M for the assembly of

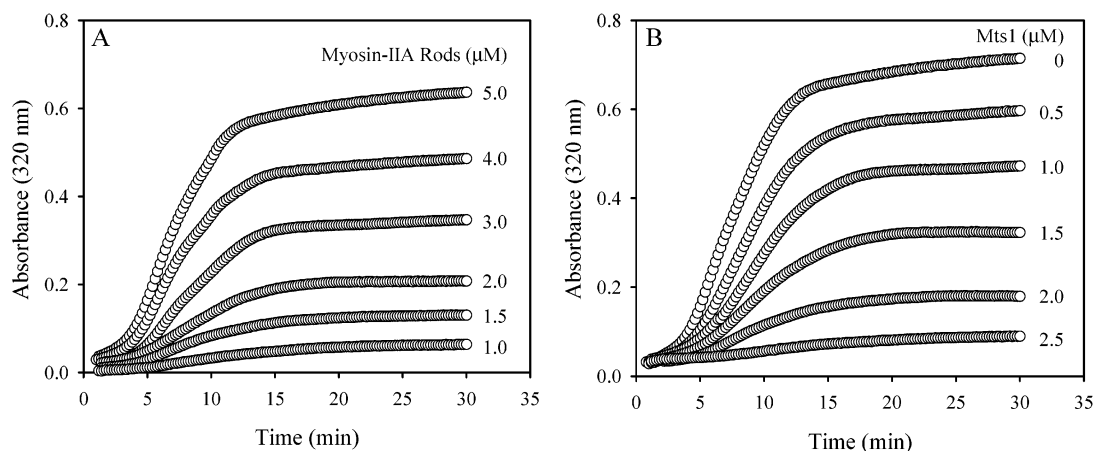


FIGURE 7: Myosin-IIA assembly kinetics in the presence of mts1. Continuous turbidometric tracings of myosin-IIA assembly. (A) Representative curves for selected myosin-IIA rod concentrations. (B) Representative curves demonstrating the effect of varying mts1 concentrations on the assembly of 5  $\mu$ M myosin-IIA. A concentration of 2.5  $\mu$ M mts1 (0.5 mts1 dimers/1 myosin-IIA rod) almost completely abolished the assembly of the myosin-IIA rods.

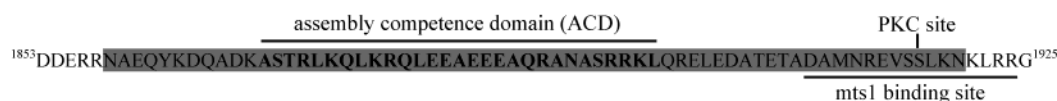


FIGURE 8: Mts1 binding site is adjacent to the assembly competence domain of human myosin-IIA. The assembly competence domain (ACD) (residues 1869–1897) is shown in bold, and the extended ACD (residues 1858–1920) is shaded in dark gray. The mts1 binding site (residues 1909–1924) is underlined, and the Ser1917 PKC phosphorylation site is marked. We propose that mts1, whose binding site partially overlaps the extended ACD, may inhibit myosin-IIA assembly by inducing partial unwinding of the coiled-coil in the ACD or extended ACD.

myosin-IIA. This finding suggests that most of the myosin-IIA should be polymerized in the cell; however, our observation that mts1 increases the critical monomer concentration  $\sim 11$ -fold suggests that mts1 may function in vivo as an effective inhibitor of myosin-IIA polymerization. An examination of the kinetics of myosin-IIA assembly in the presence of mts1 is consistent with this model. At low stoichiometries (e.g., 0.1–0.3 mts1 dimers per myosin-IIA rod), mts1 had only a small effect on the half-time for assembly and predominately affected the final extent of myosin IIA polymerization. Only at stoichiometric mts1 concentrations did we observe effects on both the half-time for assembly as well as the amount of myosin-II polymer. Although the detailed mechanisms by which mts1 modulates myosin-II polymerization remain to be addressed in future studies, our observations are consistent with a monomer sequestration model for the regulation of myosin IIA assembly by mts1.

Using a quantitative glutathione-Sepharose pull-down assay, we identified residues 1909–1924 of the myosin-IIA heavy chain as comprising the mts1 binding site. This region maps to the C-terminal tip of the  $\alpha$ -helical coiled-coil as Pro1928 marks the beginning of the nonhelical tailpiece that is at the very C-terminus of the myosin-IIA heavy chain. Our observation that mts1 binds a linear sequence of  $\sim 16$  amino acids is consistent with all other S100 family members examined to date, which have been shown to bind linear sequences of 13–22 residues in their protein targets (41–44).

The finding that mts1 binds to the C-terminal end of the  $\alpha$ -helical coiled-coil provides functional evidence that this region of the myosin-II rod is important for filament assembly and is supported by an earlier study, which found that an antibody that binds to the C-terminal 28 amino acids

of the coiled-coil inhibits filament assembly in vitro, and deletion of these residues abolishes myosin-II localization in vivo (45). It is well-established that the highly periodic myosin-II rod sequence contains a seven-residue heptad repeat pattern that is characteristic of all coiled-coil molecules, as well as a 28-residue periodicity with alternating bands of positively and negatively charged residues (46–48). These regular, periodic patches of oppositely charged residues are thought to mediate both parallel and antiparallel alignments of the myosin rod during filament assembly. However, the properties of the rod are not uniform along its length as studies have shown that it is the C-terminal domain of the rod that modulates myosin-II assembly and solubility (49, 50).

A highly conserved 29-residue sequence, termed the assembly competence domain or ACD, has been identified as a critical region for myosin-II assembly (Figure 8) (49, 50). A feature of the ACD is its unique charge profile, which is composed of four central negative charges flanked by two blocks of positive charges and which is unlike any other 28-residue repeat present in the coiled-coil of the myosin-II rod (49). In addition, the sequences immediately flanking the ACD contain a surprisingly high proportion of large apolar residues that are predicted to occupy solvent accessible positions on the coiled-coil (50). These sequences on either side of the ACD, as well as the ACD itself, have been termed the extended ACD and are predicted to form a very stable coiled-coil (50). Interestingly, the mts1 binding site overlaps the C-terminal end of the extended ACD (Figure 8). Since all S100-target complexes examined thus far indicate that each monomer binds a single polypeptide chain (41–44), we predict that each monomer in the mts1 dimer will bind only one strand on the myosin-II coiled-coil. However, since the ligand binding sites in the mts1 dimer have an antiparallel



orientation relative to one another (22), we do not expect a single mts1 dimer to bind both strands of the coiled-coil in a myosin-II monomer, but rather mts1 could cross-link two myosin-II monomers in an antiparallel orientation. Furthermore, if mts1 binds to only one strand on the myosin-II coiled-coil, this binding interaction could prevent filament assembly by inducing partial unwinding of the coiled-coil in the ACD or extended ACD.

Last, in addition to the regulation of the mts1-myosin-IIA interaction by calcium, there is a PKC phosphorylation site at Ser-1917, which is contained within the mts1 binding site on the myosin-IIA heavy chain (51) (Figure 8). Although phosphorylation by PKC is known to regulate the assembly of myosin-IIB, myosin-IIA assembly is not regulated by heavy chain phosphorylation (37, 52). We propose that myosin-IIA heavy chain phosphorylation, and in particular PKC phosphorylation, is a mechanism for regulating the binding of mts1 to myosin-IIA. This is supported by a recent study showing that a 9-fold molar excess of mts1 decreased the ability of PKC to phosphorylate the heavy chain of platelet-purified myosin-IIA by 50% (30). However, since (i) both the RLC and the heavy chain of myosin-II are PKC substrates (51, 53) and (ii) mts1 was phosphorylated by PKC in this study (30), the regulation of the mts1-myosin-IIA interaction by heavy chain phosphorylation should be reexamined in quantitative studies that also evaluate the functional consequences of myosin-IIA heavy chain phosphorylation on the ability of mts1 to promote the monomeric, unassembled state.

## ACKNOWLEDGMENT

We are grateful to Drs. Leslie Leinwand and Robert Adelstein for providing us with the cDNAs for human myosin-IIA and human myosin-IIB, respectively. We thank Drs. Michael Brenowitz, Argyris Argyrou, and Michael Ostap for helpful discussions.

## REFERENCES

- Shirinsky, V. P., Vorotnikov, A. V., Birukov, K. G., Nanaev, A. K., Collinge, M., Lukas, T. J., Sellers, J. R., and Watterson, D. M. (1993) *J. Biol. Chem.* 268, 16578–83.
- Okagaki, T., Nakamura, A., Suzuki, T., Ohmi, K., and Kohama, K. (2000) *J. Cell. Biol.* 148, 653–63.
- Donato, R. (2001) *Int. J. Biochem. Cell Biol.* 33, 637–68.
- Grigorian, M., Tulchinsky, E., Zain, S., Ebralidze, A. K., Kramerov, D. A., Kriajevska, M. V., Georgiev, G. P., and Lukanidin, E. M. (1993) *Gene* 135, 229–38.
- Ebralidze, A., Tulchinsky, E., Grigorian, M., Afanasyeva, A., Senin, V., Revazova, E., and Lukanidin, E. (1989) *Genes Dev.* 3, 1086–93.
- Nikitenko, L. L., Lloyd, B. H., Rudland, P. S., Fear, S., and Barraclough, R. (2000) *Int. J. Cancer* 86, 219–28.
- Rudland, P. S., Platt-Higgins, A., Renshaw, C., West, C. R., Winstanley, J. H., Robertson, L., and Barraclough, R. (2000) *Cancer Res.* 60, 1595–603.
- Platt-Higgins, A. M., Renshaw, C. A., West, C. R., Winstanley, J. H., De Silva Rudland, S., Barraclough, R., and Rudland, P. S. (2000) *Int. J. Cancer* 89, 198–208.
- Davies, B. R., Davies, M. P., Gibbs, F. E., Barraclough, R., and Rudland, P. S. (1993) *Oncogene* 8, 999–1008.
- Grigorian, M., Ambartsumian, N., Lykkesfeldt, A. E., Bastholm, L., Elling, F., Georgiev, G., and Lukanidin, E. (1996) *Int. J. Cancer* 67, 831–41.
- Takenaga, K., Nakamura, Y., and Sakiyama, S. (1997) *Oncogene* 14, 331–7.
- Maelandsmo, G. M., Hovig, E., Skrede, M., Engebraaten, O., Florenes, V. A., Myklebost, O., Grigorian, M., Lukanidin, E., Scanlon, K. J., and Fodstad, O. (1996) *Cancer Res.* 56, 5490–8.
- Ambartsumian, N. S., Grigorian, M. S., Larsen, I. F., Karlstrom, O., Sidenius, N., Rygaard, J., Georgiev, G., and Lukanidin, E. (1996) *Oncogene* 13, 1621–30.
- Davies, M. P., Rudland, P. S., Robertson, L., Parry, E. W., Jolicœur, P., and Barraclough, R. (1996) *Oncogene* 13, 1631–7.
- Kriajevska, M. V., Cardenas, M. N., Grigorian, M. S., Ambartsumian, N. S., Georgiev, G. P., and Lukanidin, E. M. (1994) *J. Biol. Chem.* 269, 19679–82.
- Ford, H. L., Silver, D. L., Kachar, B., Sellers, J. R., and Zain, S. B. (1997) *Biochemistry* 36, 16321–7.
- Kim, E. J., and Helfman, D. M. (2003) *J. Biol. Chem.* 278, 30063–73.
- Watanabe, Y., Usada, N., Minami, H., Morita, T., Tsugane, S., Ishikawa, R., Kohama, K., Tomida, Y., and Hidaka, H. (1993) *FEBS Lett.* 324, 51–5.
- Takenaga, K., Nakamura, Y., Sakiyama, S., Hasegawa, Y., Sato, K., and Endo, H. (1994) *J. Cell Biol.* 124, 757–68.
- Takenaga, K., Nakamura, Y., Endo, H., and Sakiyama, S. (1994) *Jpn. J. Cancer Res.* 85, 831–9.
- Spudich, J. A., and Watt, S. (1971) *J. Biol. Chem.* 246, 4866–71.
- Vallely, K. M., Rustandi, R. R., Ellis, K. C., Varlamova, O., Bresnick, A. R., and Weber, D. J. (2002) *Biochemistry* 41, 12670–80.
- Saez, C. G., Myers, J. C., Shows, T. B., and Leinwand, L. A. (1990) *Proc. Natl. Acad. Sci. U.S.A.* 87, 1164–8.
- Simons, M., Wang, M., McBride, O. W., Kawamoto, S., Yamakawa, K., Gdula, D., Adelstein, R. S., and Weir, L. (1991) *Circ. Res.* 69, 530–9.
- Phillips, C. L., Yamakawa, K., and Adelstein, R. S. (1995) *J. Muscle Res. Cell Motil.* 16, 379–89.
- Rovner, A. S., Fagnant, P. M., Lowey, S., and Trybus, K. M. (2002) *J. Cell Biol.* 156, 113–23.
- Davis, J. S. (1981) *Biochem. J.* 197, 301–8.
- Mahajan, R. K., and Pardee, J. D. (1996) *Biochemistry* 35, 15504–14.
- Gutfreund, H. (1972) *Enzymes: Physical Principles*, John Wiley & Sons Ltd, London.
- Kriajevska, M., Tarabykina, S., Bronstein, I., Maitland, N., Lomonosov, M., Hansen, K., Georgiev, G., and Lukanidin, E. (1998) *J. Biol. Chem.* 273, 9852–6.
- Kendrick-Jones, J., Smith, R. C., Craig, R., and Citi, S. (1987) *J. Mol. Biol.* 198, 241–52.
- Hodge, T. P., Cross, R., and Kendrick-Jones, J. (1992) *J. Cell Biol.* 118, 1085–95.
- Davis, J. S. (1981) *Biochem. J.* 197, 309–14.
- Sinard, J. H., and Pollard, T. D. (1990) *J. Biol. Chem.* 265, 3654–60.
- Kelley, C. A., Sellers, J. R., Gard, D. L., Bui, D., Adelstein, R. S., and Baines, I. C. (1996) *J. Cell Biol.* 134, 675–87.
- Maupin, P., Phillips, C. L., Adelstein, R. S., and Pollard, T. D. (1994) *J. Cell Sci.* 107, 3077–90.
- Murakami, N., Chauhan, V. P., and Elzinga, M. (1998) *Biochemistry* 37, 1989–2003.
- Kolega, J. (1998) *J. Cell Sci.* 111, 2085–95.
- Murakami, N., Kotula, L., and Hwang, Y. W. (2000) *Biochemistry* 39, 11441–51.
- Honer, B., Citi, S., Kendrick-Jones, J., and Jockusch, B. (1988) *J. Cell Biol.* 107, 2181–9.
- Rety, S., Sopkova, J., Renouard, M., Osterloh, D., Gerke, V., Tabaries, S., Russo-Marie, F., and Lewit-Bentley, A. (1999) *Nat. Struct. Biol.* 6, 89–95.
- Rety, S., Osterloh, D., Arie, J. P., Tabaries, S., Seeman, J., Russo-Marie, F., Gerke, V., and Lewit-Bentley, A. (2000) *Struct. Fold Des.* 8, 175–84.
- Rustandi, R. R., Baldisseri, D. M., and Weber, D. J. (2000) *Nat. Struct. Biol.* 7, 570–4.
- Inman, K. G., Yang, R., Rustandi, R. R., Miller, K. E., Baldisseri, D. M., and Weber, D. J. (2002) *J. Mol. Biol.* 324, 1003–14.
- Ikebe, M., Komatsu, S., Woodhead, J. L., Mabuchi, K., Ikebe, R., Saito, J., Craig, R., and Higashihara, M. (2001) *J. Biol. Chem.* 276, 30293–300.
- Parry, D. A. (1981) *J. Mol. Biol.* 153, 459–64.
- McLachlan, A. D., and Karn, J. (1983) *J. Mol. Biol.* 164, 605–26.
- Warrick, H. M., De Lozanne, A., Leinwand, L. A., and Spudich, J. A. (1986) *Proc. Natl. Acad. Sci. U.S.A.* 83, 9433–7.



49. Sohn, R. L., Vikstrom, K. L., Strauss, M., Cohen, C., Szent-Gyorgyi, A. G., and Leinwand, L. A. (1997) *J. Mol. Biol.* 266, 317–30.
50. Cohen, C., and Parry, D. A. (1998) *J. Struct. Biol.* 122, 180–7.
51. Conti, M. A., Sellers, J. R., Adelstein, R. S., and Elzinga, M. (1991) *Biochemistry* 30, 966–70.
52. Murakami, N., Singh, S. S., Chauhan, V. P., and Elzinga, M. (1995) *Biochemistry* 34, 16046–55.
53. Nishikawa, M., Sellers, J. R., Adelstein, R. S., and Hidaka, H. (1984) *J. Biol. Chem.* 259, 8808–14.

BI0354379